

University of Dundee

### Isomeric O-methyl cannabidiolquinones with dual BACH1/NRF2 activity

Casares Perez, Laura; Unciti-Broceta, Juan Diego; Prados, Maria Eugenia; Caprioglio, Diego; Mattoteia, Daiana; Higgins, Maureen

*Published in:*  
Redox Biology

*DOI:*  
[10.1016/j.redox.2020.101689](https://doi.org/10.1016/j.redox.2020.101689)

*Publication date:*  
2020

*Licence:*  
CC BY

*Document Version*  
Publisher's PDF, also known as Version of record

[Link to publication in Discovery Research Portal](#)

#### *Citation for published version (APA):*

Casares Perez, L., Unciti-Broceta, J. D., Prados, M. E., Caprioglio, D., Mattoteia, D., Higgins, M., Apendino, G., Dinkova-Kostova, A. T., Muñoz, E., & de la Vega, L. (2020). Isomeric O-methyl cannabidiolquinones with dual BACH1/NRF2 activity. *Redox Biology*, 37, [101689]. <https://doi.org/10.1016/j.redox.2020.101689>

#### **General rights**

Copyright and moral rights for the publications made accessible in Discovery Research Portal are retained by the authors and/or other copyright owners and it is a condition of accessing publications that users recognise and abide by the legal requirements associated with these rights.

- Users may download and print one copy of any publication from Discovery Research Portal for the purpose of private study or research.
- You may not further distribute the material or use it for any profit-making activity or commercial gain.
- You may freely distribute the URL identifying the publication in the public portal.

#### **Take down policy**

If you believe that this document breaches copyright please contact us providing details, and we will remove access to the work immediately and investigate your claim.



## Short Communication

## Isomeric O-methyl cannabidiolquinones with dual BACH1/NRF2 activity

Laura Casares<sup>a</sup>, Juan Diego Unciti-Broceta<sup>b</sup>, Maria Eugenia Prados<sup>b</sup>, Diego Caprioglio<sup>c</sup>,  
Daiana Mattoteia<sup>c</sup>, Maureen Higgins<sup>a</sup>, Giovanni Apendino<sup>c</sup>, Albena T. Dinkova-Kostova<sup>a</sup>,  
Eduardo Muñoz<sup>d,e,f,1</sup>, Laureano de la Vega<sup>a,1,\*</sup>

<sup>a</sup> Jacqui Wood Cancer Centre, Division of Cellular Medicine, School of Medicine, University of Dundee, UK

<sup>b</sup> Emerald Health Biotechnology, Córdoba, Spain

<sup>c</sup> Dipartimento di Scienze Del Farmaco, Università Del Piemonte Orientale, Novara, Italy

<sup>d</sup> Instituto Maimónides de Investigación Biomédica de Córdoba, Spain

<sup>e</sup> Departamento de Biología Celular, Fisiología e Inmunología, Universidad de Córdoba, Spain

<sup>f</sup> Hospital Universitario Reina Sofía, Córdoba, Spain



## ARTICLE INFO

## Keywords:

Cannabidiol derivative/ NRF2/ BACH1/  
HMOX1/ neurodegenerative diseases

## ABSTRACT

Oxidative stress and inflammation in the brain are two key hallmarks of neurodegenerative diseases (NDs) such as Alzheimer's, Parkinson's, Huntington's and multiple sclerosis. The axis NRF2-BACH1 has anti-inflammatory and anti-oxidant properties that could be exploited pharmacologically to obtain neuroprotective effects. Activation of NRF2 or inhibition of BACH1 are, individually, promising therapeutic approaches for NDs. Compounds with dual activity as NRF2 activators and BACH1 inhibitors, could therefore potentially provide a more robust antioxidant and anti-inflammatory effects, with an overall better neuroprotective outcome. The phytocannabinoid cannabidiol (CBD) inhibits BACH1 but lacks significant NRF2 activating properties. Based on this scaffold, we have developed a novel CBD derivative that is highly effective at both inhibiting BACH1 and activating NRF2. This new CBD derivative provides neuroprotection in cell models of relevance to Huntington's disease, setting the basis for further developments *in vivo*.

## 1. Introduction

Cells are continuously exposed to reactive oxygen species (ROS) from both exogenous and endogenous sources. To counteract the potential harmful effects of ROS, cells have evolved constitutive (housekeeping) as well as inducible antioxidant systems that regulate redox homeostasis. The master regulator of the inducible antioxidant responses is the transcription factor NF-E2-related factor 2 (NRF2), a member of the cap'n'collar basic region leucine zipper (CNC-bZip) transcription factor family. NRF2 binds to Antioxidant Response Elements (ARE) in the promoters of its target genes, many of which encode antioxidant and other cytoprotective proteins, and triggers their expression [1]. BTB And CNC Homology 1 (BACH1) is a transcriptional repressor, also belonging to the CNC-bZip family, that competes with NRF2 for binding to ARE sites located at the promoter of oxidative stress responsive genes, such as heme oxygenase 1 (HMOX1) [2].

In homeostatic conditions, NRF2 binds to its negative regulator

Kelch-like ECH-associated protein 1 (KEAP1) in the cytoplasm, and is targeted for ubiquitination and subsequent proteasomal degradation by the Cullin3-containing E3-ligase complex [3]. When cells are exposed to oxidants or electrophiles, KEAP1 is disabled, allowing for accumulation and translocation of *de novo* synthesized NRF2 to the nucleus [4] while BACH1 is exported out of the nucleus and degraded [5]. Only a subset of NRF2 target genes are regulated by BACH1, HMOX1 being the best characterized one. It encodes heme oxygenase 1 (HMOX1), an enzyme which catalyzes the rate-limiting reaction in heme degradation [6]. It is generally accepted that BACH1 and NRF2 work together to regulate the expression of HMOX1, with the negative effect of BACH1 dominating over the positive effect of NRF2. This means that BACH1 needs to be displaced from the HMOX1 promoter in order for NRF2 to bind and induce its expression [7]. However, we and others have shown that HMOX1 induction can be BACH1-dependent, but NRF2-independent [8, 9], suggesting that the regulation of HMOX1 is most likely cell type- and context-dependent.

\* Corresponding author.

E-mail address: [l.delavega@dundee.ac.uk](mailto:l.delavega@dundee.ac.uk) (L. de la Vega).

<sup>1</sup> Equal senior authorship.

HMOX1 has anti-inflammatory properties [10,11], and its knockout in mouse models leads to the development of chronic inflammation [12,13]. The antioxidant role of HMOX1 is largely attributed to its capacity to degrade heme into biliverdin, which is rapidly converted to the antioxidant bilirubin, free iron, and carbon monoxide [14,15]. Furthermore, various studies have shown that overexpression of HMOX1 protects cells from oxidative damage and neurotoxicity [11,16]. Oxidative stress and inflammation in the brain are two key hallmarks of neurodegenerative diseases (NDs) such as Alzheimer's, Parkinson's, Huntington's and multiple sclerosis (MS). Thus, BACH1 inhibitors, by inducing HMOX1, could be developed as neuroprotective agents.

Despite their therapeutic potential, so far only very few BACH1 inhibitors have been reported. The compound most widely used to inhibit BACH1 is the oxidized form of its endogenous ligand heme. Hemin binds to BACH1, impairing its binding to DNA, promoting its nuclear export and its degradation via the E3 ligase Fbxo22 [17–19]. Hemin is a very potent inhibitor, but its clinical use is limited by the toxic nature of free heme [20]. Other BACH1 inhibitor is the natural non-psychotropic phytocannabinoid cannabidiol (CBD). We have shown that CBD targets BACH1 for degradation and, consequently, induces *HMOX1* [9]. CBD is neuroprotective in a murine MS model [21] and has been tested in various animal and cell models of other NDs [22], and some of its beneficial effects could indeed be related to its inhibitory effect on BACH1. Another reported BACH1 inhibitor is the synthetic compound HPP-4382 [23] that, to the best of our knowledge, has not yet been tested in any disease models.

Pharmacological activation of NRF2 is also beneficial in most pathologies with underlying oxidative stress and inflammation [24]. Most compounds that stabilise NRF2 are either electrophilic molecules that covalently modify certain cysteine residues in KEAP1, impairing its activity [25], or inhibitors that interfere with the binding between NRF2 and KEAP1 [26]. Stabilisation of NRF2 triggers the transcription of multiple enzymes involved in scavenging ROS and in generating antioxidant molecules like glutathione [27,28] while leading to a reduction of pro-inflammatory cytokines such as IL-6 [29,30]. Thus NRF2 activators have also been studied for their potential neuroprotective effect [31]. In fact, the activation of the NRF2 pathway has been shown to be neuroprotective in various models of NDs such as MS and Huntington disease (HD) [32,33]. HD is caused by a mutation in the huntingtin (HTT) gene; this mutant HTT tends to form aggregates that lead to the dysfunction and eventual death of neurons within the striatum [34]. HD presents high levels of oxidative stress, brain inflammation and impaired NRF2 activity [35], and NRF2 activation has been shown to repress proinflammatory processes in preclinical HD models [35]. Furthermore, treatment with the NRF2 activator dimethyl fumarate (DMF) resulted in improved motor function in a mouse HD model [36].

While NRF2 activators induce the expression of many cytoprotective genes, BACH1 inhibitors activate only a few, although they are extremely potent at inducing *HMOX1*. Thus, the individual knockdown of KEAP1 (leading to constitutive NRF2 activation) or BACH1 in HaCaT cells induced the expression of *HMOX1* by 2.3- and 136-fold, respectively, whereas the combined knockdown of KEAP1 and BACH1 resulted in a 388-fold increase of *HMOX1* mRNA [37]. Consequently, complementing NRF2 activation with BACH1 inhibition would result in a highly robust anti-inflammatory and antioxidant response, and potentially a better therapeutic effect.

Cannabidiol has sparked attention due to its therapeutic potential, and there is considerable interest in synthesizing new CBD derivatives with improved pharmacological and clinical properties. In this study, we report the identification of a novel CBD derivative that is highly effective at both inhibiting BACH1 and activating NRF2, and show its cytoprotective efficacy in cell models of relevance to Huntington's disease.

## 2. Materials and methods

### 2.1. Cell culture

The following cell lines were used in this study: HaCaT, THP1, SH-SY5Y, Hepa 1c1c7, A549 and Q7/Q111. HaCaT cells have been validated by STR profiling and were routinely tested for mycoplasma. HaCaT-ARE-Luc cells were generated as described previously [38]. HaCaT NRF2-KO cells were produced using the CRISPR-Cas9 system as described [9]. CRISPR-edited HaCaT BACH1-KO and HaCaT NRF2-KO/BACH1-KO cells were generated by transfecting either HaCaT WT or HaCaT NRF2-KO cells with two different pLentiCRISPR-v2 (a gift from Dr Feng Zhang, Addgene plasmid #52961) containing each one a guide RNA against the first exon and the second exon of BACH1, respectively (5'-CGATGTCACCATCTTTGTGG-3', 5'-GACTCTGAGACG GACACCGA-3'). All CRISPR-edited cell lines were selected for two days using puromycin, cells were clonally selected by serial dilution and positive clones were identified, as previously described [39]. Control cells, referred to as HaCaT wild type (HaCaT WT), are the pooled population of surviving cells transfected with an empty pLentiCRISPRv2 vector treated with puromycin. THP1, SH-SY5Y, Hepa-1c1c7 and A549 cells were obtained from ATCC and were routinely tested for mycoplasma. Clonal striatal cell lines established from E14 striatal primordia of *Hdh*<sup>Q111/Q111</sup> (mutant) and *Hdh*<sup>Q7/Q7</sup> (wild-type) knock-in mouse littermates and immortalized as previously described [40]. Cell lines were grown in RPMI (HaCaT, THP1), DMEM (A549), DMEM/F12 (SH-SY5Y) or alpha-MEM (Hepa-1c1c7) with 10% FBS at 37 °C and 5% CO<sub>2</sub>. Striatal Q7 and Q111 cells were maintained in DMEM containing 25 mM D-glucose, 1 mM L-glutamine, 10% fetal bovine serum (FBS), 1 mM sodium pyruvate, and 400 µg/mL Geneticin (Invitrogen, Carlsbad, CA) and were incubated at 33 °C with 5% CO<sub>2</sub>.

### 2.2. Antibodies and reagents

Antibodies recognizing Beta-Actin (C-4) and anti-BACH1 (F-9) were obtained from Santa Cruz Biotechnology (Dallas, Texas, USA). anti-NRF2 (D1Z9C) was obtained from Cell Signalling Technology (Danvers, MA, USA) and anti-HMOX1 was purchased from Biovision (San Francisco, CA, USA). The siRNAs used as control or against KEAP1 were the SMART pool: ON-Target Plus from Dharmacon (Lafayette, CO, USA). CBD (Fig. 1B (1)) was isolated from the Cannabis strain Carmagnola [41].

### 2.3. Synthesis of the CBD derivatives

**O-Methyl para-cannabidiolquinone (Compound 2):** To a cooled (ice bath) solution of cannabidiolquinone (Fig. 1B (4)) (1.87 g, 5.69 mmol) [42] in DMF (19 mL), solid NaHCO<sub>3</sub> (0.95 g, 11.31 mmol) was added. After stirring for 10 min, methyl iodide (1.75 g, 28.11 mmol) was added, and the resulting mixture was stirred overnight at room temperature. The reaction was worked up by dilution with water (75 mL) and EtOAc (75 mL), and, after a 5 min stirring, the two layers were separated. The lower organic layer was washed with water (2 × 25 mL), dried (Na<sub>2</sub>SO<sub>4</sub>) and evaporated to obtain a dark oily residue, that was purified by gravity column chromatography on silica gel, using an EtOAc gradient in hexane (from 1:99 to 4:96). 960 mg (49%) O-methyl para-cannabidiolquinone were obtained as a red oil. <sup>1</sup>H NMR (300 MHz, CDCl<sub>3</sub>) δ = 6.37 (t, J = 1.5, 1H), 5.10 (s, 1H), 4.59–4.48 (m, 2H), 3.87 (s, 3H), 3.82–3.67 (m, 1H), 2.70 (td, J = 11.1, 10.7, 3.2, 1H), 2.36 (dd, J = 10.2, 6.2, 1.5, 2H), 2.29–2.10 (m, 1H), 2.07–1.91 (m, 1H), 1.81–1.59 (m, 3H), 1.69 (s, 3H), 1.64 (s, 3H), 1.57–1.42 (m, 2H), 1.42–1.24 (m, 4H), 0.97–0.83 (m, 3H).

**O-Methyl ortho-cannabidiolquinone (Compound 3):** To a solution of O-methyl cannabidiol (Fig. 1B (5)) [43] (2.25 g, 6.85 mmol) in EtOAc (150 mL), SIBX (42.7%, 13.5 g, 20.59 mmol) was added, and the mixture was stirred at room temperature for 24 h. The reaction was

worked up by filtration, and the filtrate was washed with sat.  $\text{NaHCO}_3$  ( $3 \times 100$  mL), dried ( $\text{Na}_2\text{SO}_4$ ), and evaporated. A dark red oil was obtained, that was purified by gravity column chromatography (silica gel, EtOAc/hexanes 4:96 as eluant) to afford 1.19 g (51%) of O-methyl *ortho*-cannabidiolquinone as a dark red oil.  $^1\text{H}$  NMR (300 MHz,  $\text{CDCl}_3$ )  $\delta$  = 6.84 (s, 1H), 5.08 (s, 1H), 4.61–4.51 (m, 2H), 3.89 (s, 3H), 3.74–3.61 (m, 1H), 2.76–2.62 (m, 1H), 2.35 (t,  $J$  = 7.7, 2H), 2.27–2.10 (m, 1H), 2.03–1.91 (m, 1H), 1.80–1.59 (m, 3H), 1.66 (s, 3H), 1.63 (s, 3H), 1.49 (m, 2H), 1.39–1.24 (m, 4H), 0.95–0.82 (m, 3H).

#### 2.4. Quantitative real time PCR (rt-qPCR)

Samples were lysated and homogenised using the QIAshredder (Qiagen, Hilden, Germany) and RNA was extracted using RNeasy kit (Qiagen). 500 ng of RNA per sample was reverse-transcribed to cDNA using Omniscript RT kit (Qiagen) supplemented with RNase inhibitor (Invitrogen, Waltham, MA, USA) according to the manufacturer's instructions. Resulting cDNA was analysed using TaqMan Universal Master Mix II (Life Technologies, Carlsbad, CA, USA). Gene expression was determined by the comparative  $\Delta\Delta\text{CT}$  method, using a QuantStudio 7 Flex qPCR machine. All experiments were performed at least in triplicates and data were normalised to the housekeeping gene HPRT1. The TaqMan probes used are:

HPRT1 Hs02800695\_m1 HPRT1 TaqMan(s).

HMOX1 Hs01110250\_m1 HMOX1 TaqMan(s).

AKR1B10 Hs00252524\_m1 AKR1B10 TaqMan (s).

NQO1 Hs01045993\_g1 NQO1 TaqMan (m).

#### 2.5. Cell lysis and Western blot protocol

Cells were washed and harvested in ice-cold phosphate-buffered saline (PBS) and lysed in RIPA buffer supplemented with phosphate and protease inhibitors [50 mM Tris- HCl pH 7.5, 150 mM NaCl, 2 mM EDTA, 1% NP40, 0.5% sodium deoxycholate, 0.5 mM  $\text{Na}_3\text{VO}_4$ , 50 mM NaF, 2  $\mu\text{g/mL}$  leupeptine, 2  $\mu\text{g/mL}$  aprotinin, 0.05 mM pefabloc]. Lysates were sonicated for 15 s at 20% amplitude and then cleared by centrifugation for 15 min at 4 °C. Protein concentration was established using the BCA assay (Thermo Fisher Scientific, Waltham, MA, USA). Lysate was mixed with SDS sample buffer and boiled for 7 min at 95 °C. Equal amounts of protein were separated by SDS-PAGE, followed by semidry blotting to a polyvinylidene difluoride membrane (Thermo Fisher Scientific). After blocking of the membrane with 5% (w/v) TBST non-fat dry milk, primary antibodies were added overnight. Appropriate secondary antibodies coupled to horseradish peroxidase were detected by enhanced chemiluminescence using Clarity™ Western ECL Blotting Substrate (Bio-Rad, Hercules, CA, USA). Resulting protein bands were quantified and normalised to each lane's loading control using the ImageStudio software (LI-COR).

#### 2.6. siRNA cell transfections

The day before the transfection cells were plated into 6-well plates to 70–90% confluency. The siRNA and Lipofectamine RNAiMAX (Invitrogen, Carlsbad, CA, USA) were individually diluted in Opti-MEM (Life Technologies) and incubated for 10 min at room temperature. Diluted siRNA was added to the diluted Lipofectamine solution (1:1 ratio) and further incubated for 15 min. The complex was added to the cells and incubated in a humidified incubator at 37 °C and 5%  $\text{CO}_2$  for 36 h prior treatment and lysis.

#### 2.7. Cell viability assays

To assess cell viability of HaCaT cells after drug treatment we performed an Alamar Blue assay. One day before the experiment, HaCaT cells were seeded into a 96-well plate to 50–60% confluency. Cells were treated with the corresponding compounds for 16 h and Alamar Blue

(Thermo Fisher Scientific) was added to the wells. After 4 h of incubation at 37 °C the fluorescence was measured using a microplate reader (Spectramax m2) and viability was calculated relative to the DMSO treated control. For the *in vitro* HD model we used  $\text{STHdh}^{Q7/Q7}$  and  $\text{STHdh}^{Q111/Q111}$  cells, which express either a wild type or a mutated form of the huntingtin protein [44]. These cells were cultured at 33 °C and 5%  $\text{CO}_2$  in DMEM supplemented with 10% FBS, 2 mM L-glutamine and 1% (v/v) penicillin/streptomycin (Epub 2000/11/25).  $\text{STHdh}^{Q7/Q7}$  and  $\text{STHdh}^{Q111/Q111}$  cells ( $10^4$  cells/well) were seeded in DMEM supplemented with 10% FBS in 96 well plates incubated with increased concentrations of compound 2 and treated with 3-NP at 10 mM (#N5636, Sigma). Then, 3-NP-induced cytotoxicity was measured by fluorescence using the dye YOYO-1 (#Y3601, Life Technologies). Treated cells were placed in an Incucyte FLR imaging system and the YOYO-1 fluorescence was measured after several time points. Object counting analysis is performed using the Incucyte FLR software to calculate the total number of YOYO-1 fluorescence positive cells and total DNA containing objects (endpoint). The cytotoxicity index is calculated by dividing the number of YOYO-1 fluorescence positive objects by the total number of DNA containing objects for each treatment group.

#### 2.8. Luciferase assays

HaCaT-ARE-Luc cells were stimulated with the indicated compounds for either 6h (one time-point) or for the indicated time points (kinetic). After the treatment the cells were washed twice in PBS and lysed in 25 mM Tris-phosphate pH 7.8, 8 mM  $\text{MgCl}_2$ , 1 mM DTT, 1% Triton X-100, and 7% glycerol during 15 min at room temperature in a horizontal shaker. After centrifugation, luciferase activity in the supernatant was measured using a GloMax 96 microplate luminometer (Promega) following the instructions of the luciferase assay kit (Promega, Madison, WI, USA). Results are expressed in RLU over control untreated cells.

#### 2.9. ROS determination

The intracellular accumulation of ROS was detected using 2',7'-dihydrofluorescein-diacetate (DCFH-DA). HaCaT cells ( $15 \times 10^3$  cells/well) were cultured in a 96-well plate in DMEM supplemented with 10% FBS until cells reached 80% confluence. Cells were pre-treated with the compounds for 30 min and treated with 0.4 mM Tert-butyl-hydroperoxide (TBHP). At the indicated time points, the cells were incubated with 10  $\mu\text{M}$  DCFH-DA in the culture medium at 37 °C for 30 min. Then, the cells were washed with PBS at 37 °C and the production of intracellular ROS was measured by DCF fluorescence and detected using the Incucyte FLR software. The data were analysed by the total green object integrated intensity (GCU $\mu\text{m}^2 \times \text{Well}$ ) of the imaging system IncuCyte HD (Sartorius, Göttingen, Germany).

#### 2.10. NQO1 activity assay

Cells were lysed in digitonin (0.8 g/L in 2 mM EDTA, pH 7.8), and the lysates were subjected to centrifugation at 4 °C (15,000 $\times$ g for 10 min). The enzyme activity of NQO1 was measured in lysate supernatants using menadione as a substrate as previously described [45].

#### 2.11. Statistical analysis

Most experiments were repeated 3–5 times with multiple technical replicates to be eligible for the indicated statistical analyses. Data were analysed using Graphpad Prism statistical package. All results are presented as mean  $\pm$  SD unless otherwise mentioned. When applicable, the differences between groups were determined by either one-way ANOVA or 2-way ANOVA. A P value of <0.05 was considered significant. \* $P \leq 0.05$ , \*\* $P \leq 0.01$ , \*\*\* $P \leq 0.001$ .



### 3. Results and discussion

#### 3.1. Identification of CBD derivatives that activate ARE-dependent gene expression

We have recently shown that CBD is a potent BACH1 inhibitor, but a very weak NRF2 activator in HaCaT cells [9]. In search for CBD derivatives with higher potency in activating NRF2, we screened a library of semi-synthetic cannabidiol quinone derivatives in the NRF2 reporter cell line HaCaT ARE-Luc. This reporter cell line responds well to NRF2 activation (after treatment with the NRF2 activator sulforaphane), but not to BACH1 inhibition (treatment with the BACH1 inhibitor hemin) (Suppl. Fig. S1A), thus discriminating between both activities. We identified the isomeric quinoids *O*-methyl *para*-cannabidiolquinone (hereinafter referred to as compound 2) and *O*-methyl *ortho*-cannabidiolquinone (hereinafter referred to as compound 3) as reporter activators in a concentration-dependent manner (Fig. 1A).

Compared to CBD, compounds 2 and 3 are characterized by the oxidation of the resorcinyl core to a methoxylated quinone moiety (Fig. 1B). Early studies preceding the discovery of NRF2 had shown that among diphenols, only 1,2 diphenols (catechols) and 1,4-diphenols (hydroquinones), but not 1,3-diphenols (resorcinols), were inducers of the cytoprotective enzyme NAD(P)H:quinone oxidoreductase 1 (NQO1) [46] which is now widely accepted as a classical NRF2-regulated protein [47]. This realization established that oxidative lability among diphenols, i.e. their ability to form quinones in the presence of oxygen, was essential for inducer activity. This notion was further strengthened by the finding of a linear correlation between the NQO1 inducer activity and the ability to release an electron among inducers of different classes, including diphenols, phenylpropanoids, and flavonoids [48]. Subsequent work showed that the stronger the electron-attracting property of a quinone, the greater its inducing potency [49], implicating oxidation of cysteine sensors of KEAP1 by quinones in the mechanism of NRF2 activation. Experiments using recombinant KEAP1 in the presence or absence of Cu<sup>++</sup> and oxygen firmly established that oxidizable diphenols are not NRF2 activators themselves, but their corresponding quinones are the ultimate inducers [50].

Diphenols have been proposed as pro-drugs to combat oxidative stress based on the concept that such compounds are chemically converted to their active quinone forms by the oxidative environment that they are designed to protect against [51]. It is therefore highly likely that the NRF2 inducer property of these compounds is conferred by their quinone functionalities.

To validate the results from the screen, we first compared the effect of compound 2 and 3 to that of CBD on the protein levels of BACH1 and NRF2 in HaCaT cells. Both compounds were more potent than CBD at stabilising NRF2, fully retaining the ability to reduce the levels of BACH1 (Fig. 1C).

#### 3.2. Validation of compound 2 as a dual BACH1 inhibitor and NRF2 inducer

To further characterise the effect of compound 2 and compound 3 on BACH1 and NRF2, we compared them with the BACH1 inhibitor hemin and the NRF2 activator sulforaphane (SFN) (Fig. 1D and quantification in Suppl. Fig. S1B). Both compound 2 and compound 3 reduced BACH1 protein levels. Consistent with the negative regulation of HMOX1 expression by BACH1, treatment with compound 2 or compound 3 increased the protein levels of HMOX1. When compared with hemin, both compounds at a concentration of 10 µM showed similar efficacy in decreasing BACH1 levels as that of hemin at a concentration of 1 µM. Furthermore, both compound 2 and compound 3 stabilised NRF2 in a

concentration-dependent manner, and this effect was comparable to the effect of SFN. As compound 3 was more toxic (Suppl. Fig. S1C) and less stable at room temperature (Suppl. Fig. S1D), we focused on compound 2 for the rest of this study.

To confirm that the activation of NRF2 by compound 2 was not limited to HaCaT cells, we tested this compound in Hepa1c7 cells, a cell line widely used to study NRF2 activation [52]. Our results showed that in Hepa1c7 cells, compound 2 stabilised NRF2 and induced HMOX1 (Suppl. Fig. S1E). Compound 2 also dose-dependently induced the enzyme activity of the classical NRF2 target, NAD(P)H:quinone oxidoreductase 1 (NQO1) (Suppl. Fig. S1F).

We have previously shown that in HaCaT cells, *HMOX1* expression is an excellent surrogate for BACH1 activity as it is regulated primarily by BACH1 and not by NRF2, while *AKR1B10* is a surrogate for NRF2 activity and does not respond to BACH1 modulation [9] (also see Suppl. Fig. S2). To further validate compound 2 as a dual BACH1 inhibitor and an NRF2 inducer, we analysed its effect on the expression of these surrogate markers in HaCaT cells. As shown in Fig. 1E, compound 2 was more potent than CBD at inducing *HMOX1* and *AKR1B10* expression. As expected, SFN induced the expression of *AKR1B10*, but not *HMOX1*, whereas hemin induced *HMOX1*, but not *AKR1B10* expression. Additionally, we also analysed the effect of compound 2 on genes that, based on the literature were regulated by both NRF2 and BACH1, such as NQO1, GCLC and p62. We first tested that in our cell system these genes were actually regulated by both factors (Suppl. Fig. S1G), and once validated, we showed that compound 2 activated all three genes, although with different efficiency (Suppl. Fig. S1H).

#### 3.3. Characterisation of the effect of compound 2 on NRF2 and BACH1

To further characterise the effect of compound 2, we tested whether in a similar way to CBD, the compound 2-mediated induction of *HMOX1* was dependent on BACH1. As observed in Fig. 2A, the ability of both compound 2 and hemin to induce *HMOX1* was abolished in BACH1-KO cells (validation of BACH1-KO cells in Suppl. Fig. S2A and Suppl. S2B). On the other hand, BACH1 knockout did not impair the effect of compound 2 inducing *AKR1B10* (Fig. 2B) or stabilising NRF2 (Fig. 2C), showing that NRF2 activation by compound 2 does not depend on BACH1. Similarly, the inhibition of BACH1 by compound 2 was still evident in NRF2-KO cells (Fig. 2D), indicating that the two effects of compound 2 are independent (validation of NRF2-KO cells in Suppl. Fig. S2C and Suppl. Fig. S2D).

Next, we compared the kinetics of *HMOX1* and *AKR1B10* expression in response to compound 2, hemin and SFN in WT and NRF2-KO cells (Fig. 3A, B and 3C). Compound 2 increased *HMOX1* mRNA levels in an NRF2-independent manner, with similar kinetics as hemin; starting as early as 2 h and reaching its peak around 8 h (Fig. 3A and C). As previously observed, SFN induced *HMOX1* very weakly at the 8-h time point (Fig. 3B). On the other hand, compound 2 induced *AKR1B10* expression in an NRF2-dependent manner with similar kinetics as SFN, starting around 4 h and reaching its peak around 8 h (Fig. 3A and B). As expected, hemin did not induce *AKR1B10* (Fig. 3C). These results further confirm that compound 2 has dual activity targeting both BACH1 and NRF2.

Based on the strong effect of compound 2 increasing NRF2 levels, we hypothesise that this stabilisation must be a consequence of impairing the activity of its main regulator KEAP1. To test this possibility, we compared the effect of compound 2 on NRF2 levels in HaCaT cells treated with either siRNA control or an siRNA against KEAP1. The stabilisation of NRF2 induced by compound 2 was clearly impaired in KEAP1-silenced cells (Fig. 3D and Suppl. Fig. S3A). We also tested compound 2 in the lung cancer cell line A549 bearing a loss-of-function

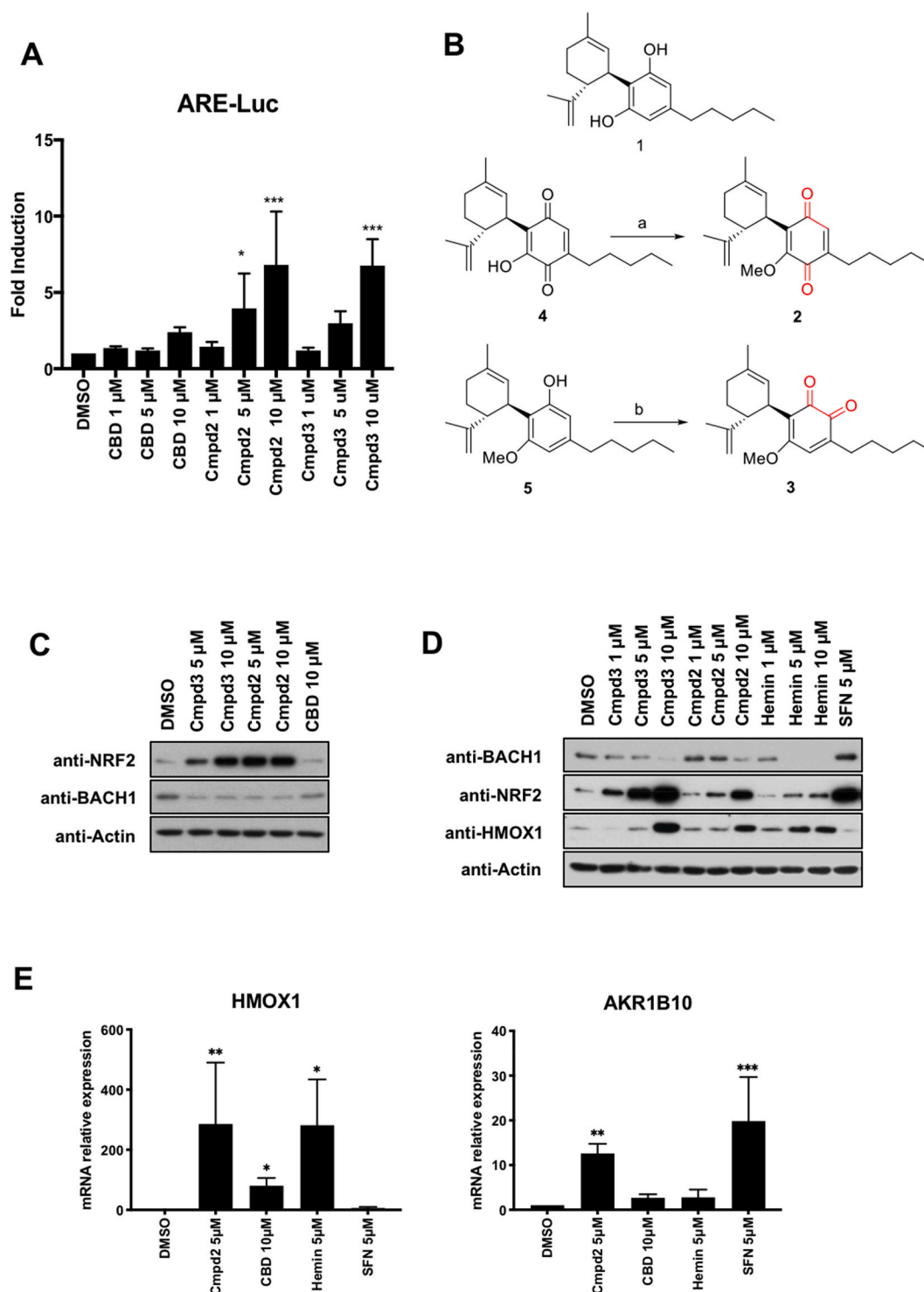


**Fig. 1.** Screening of CBD derivatives and characterization of compound 2 as a BACH1 inhibitor and NRF2 inducer. **A)** HaCaT-ARE-Luc cells were treated with either DMSO or increasing concentrations of CBD, compound 2 (Cmpd2) or compound 3 (Cmpd3) for 6 h. Luciferase activity was measured in the cell lysates and expressed as RLU ( $\times 10^4$ ). Data represent means  $\pm$  SD ( $n = 4$ ) and are expressed relative to untreated cells. \* $P \leq 0.05$ , \*\* $P \leq 0.01$ , \*\*\* $P \leq 0.001$ . **B)** Schematic representation of the synthesis of the isomeric methoxyquinones 2 (compound 2) and 3 (compound 3) from 1 (CBD). (a): MeI, NaHCO<sub>3</sub>, DMF, 49%; (b) SIBX, EtOAc, 51%. **C)** HaCaT cells were incubated with either DMSO, compound 3 (Cmpd3), compound 2 (Cmpd2) or CBD. Three hours later, cells were lysed and samples were analysed by Western Blot. **D)** HaCaT cells were incubated with either DMSO, or increasing concentrations of compound 3 (Cmpd3), compound 2 (Cmpd2), hemin or sulforaphane (SFN). Three hours later, cells were lysed and levels of BACH1, NRF2, HMOX1 and Actin were analysed by Western Blot. A representative blot is shown; the corresponding quantifications of BACH1, NRF2 and HMOX1 protein levels are shown in Suppl. Fig. S1A. **E)** HaCaT cells were treated with either DMSO, compound 2 (5  $\mu$ M), CBD (10  $\mu$ M), Hemin (5  $\mu$ M) or SFN (5  $\mu$ M) for 8 h. The mRNA levels of *HMOX1* and *AKR1B10* were quantified by real-time PCR and the data were normalised using *HPRT1* as an internal control. Data represent means  $\pm$  SD ( $n = 3$ ) and are expressed relative to the DMSO sample. Statistical analysis was performed against the DMSO sample. \* $P \leq 0.05$ , \*\* $P \leq 0.01$ , \*\*\* $P \leq 0.001$ .

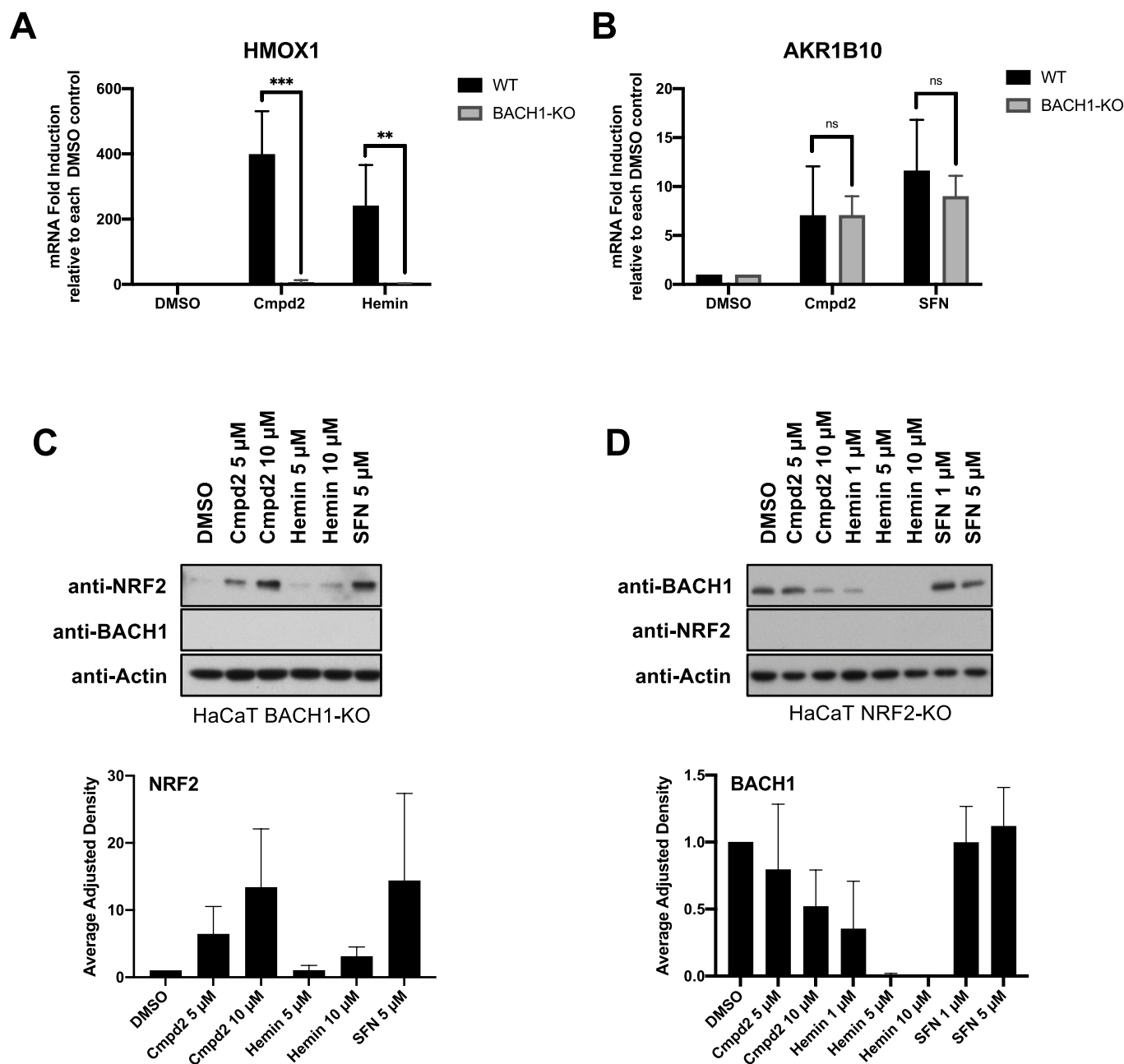


**Fig. 2.** Compound 2-mediated NRF2 induction and BACH1 inhibition are not interdependent. **A)** HaCaT WT and BACH1-KO cells were treated for 8 h with DMSO, compound 2 (10  $\mu$ M) or Hemin (10  $\mu$ M). Cells were lysed and *HMOX1* mRNA levels were quantified ( $n = 3$ ). To compare the *HMOX1* induction upon compound 2 or Hemin treatment in each cell line, the levels of *HMOX1* in either treated WT or treated BACH1-KO samples were compared against the basal level of *HMOX1* in DMSO WT or DMSO BACH1-KO respectively (*HMOX1* levels in DMSO samples were set in both cases as 1).  $**P \leq 0.01$ ,  $***P \leq 0.001$ . **B)** HaCaT WT and BACH1-KO cells were treated as indicated in A. Cells were lysed and *AKR1B10* mRNA levels were quantified by real-time PCR and the data were normalised using *HPRT1* as an internal control ( $n = 3$ ). As described in A, *AKR1B10* levels in DMSO WT and BACH1-KO samples were set in both cases as 1. **C)** HaCaT BACH1-KO cells were incubated with either DMSO or different concentrations of compound 2, Hemin or SFN. After 3 h, cells were harvested and lysates were analysed by Western Blot. Upper panel is a representative Western blot and the bottom panel shows the quantification of NRF2 protein levels against the loading control actin. Data represent means  $\pm$  SD ( $n = 3$ ) and are expressed relative to the DMSO treated samples. **D)** HaCaT NRF2-KO cells were treated and harvested as described in C and samples were analysed by Western Blot. Upper panel is a representative Western blot and the bottom panel shows the quantification of BACH1 protein levels against the loading control actin. Data represent means  $\pm$  SD ( $n = 3$ ) and are expressed relative to the DMSO samples.

mutation in KEAP1, and found that the NRF2 levels were not significantly changed by compound 2 (Suppl. Fig. S3B). Collectively, these results suggest that NRF2 activation by compound 2 requires KEAP1, and is independent of its effect on BACH1.

#### 3.4. Compound 2 protects against oxidative stress in cell-based models

The characterization of the effect of compound 2 on BACH1 and NRF2 was performed in HaCaT cells because this is a validated model where we can individually assess the compound activity on BACH1 and NRF2. However, to answer whether compound 2 could have a therapeutic benefit in NDs, we used two cell lines of relevance to

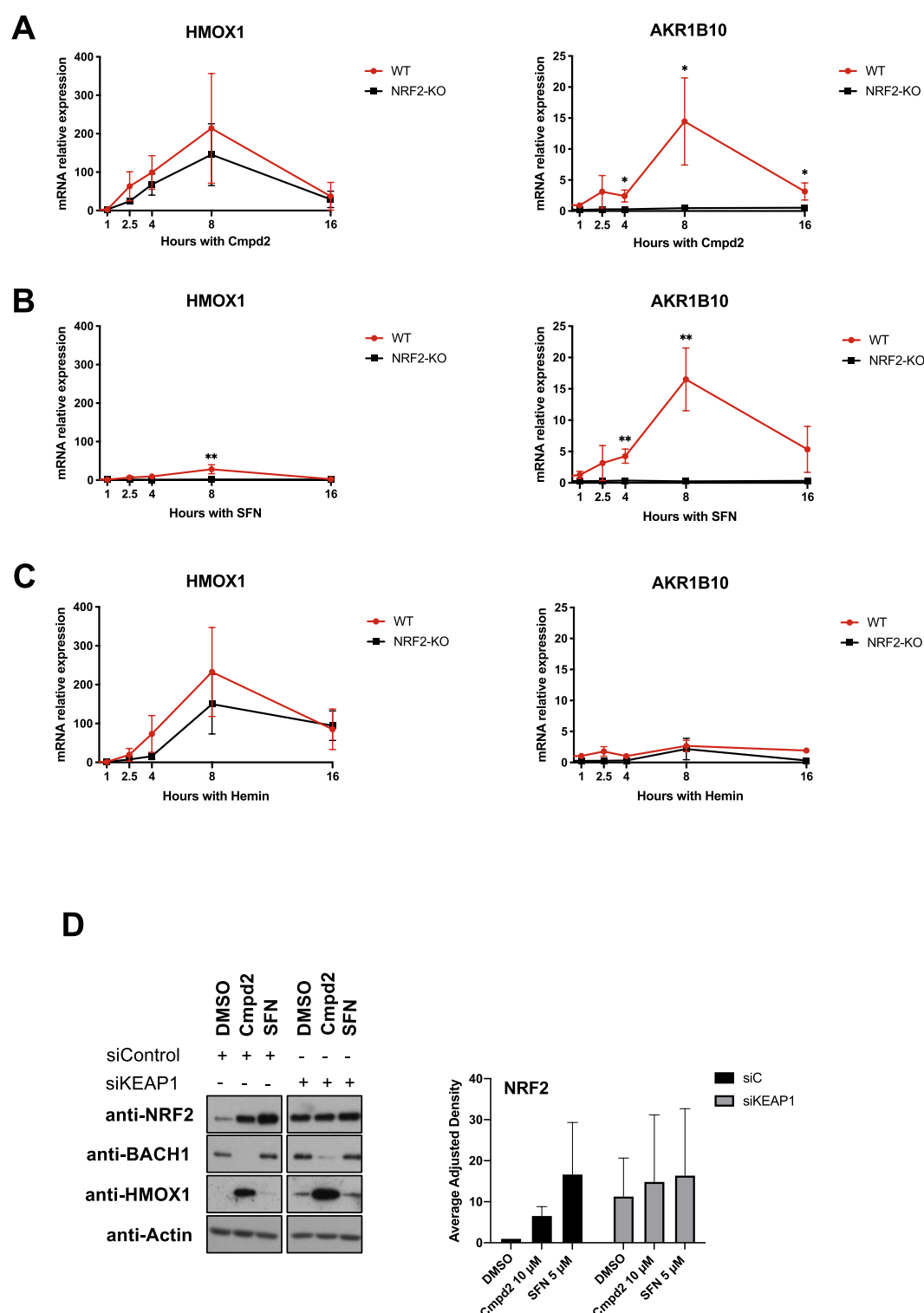


**Fig. 3.** Compound 2 inhibits BACH1 in a NRF2 and KEAP1 independent manner, and stabilizes NRF2 in a KEAP1-dependent manner. **A)** HaCaT WT and NRF2-KO cells were treated with compound 2 (10  $\mu$ M) and were harvested after 1, 2:30, 4, 8 or 16 h. Samples were lysed and *HMOX1* (left panel) or *AKR1B10* (right panel) mRNA levels were quantified by real-time PCR using HPRT1 as an internal control. *HMOX1* and *AKR1B10* levels in DMSO samples were set in both cell lines as 1 with the purpose of comparing the induction after compound 2 treatment in WT and NRF2-KO cells. Data represent means  $\pm$  SD (n = 3). \*P  $\leq$  0.05, \*\*P  $\leq$  0.01 **B)** HaCaT WT and NRF2-KO cells were treated with SFN (5  $\mu$ M) for 1, 2:30, 4, 8 or 16 h mRNA *HMOX1* and *AKR1B10* levels were analysed as described in A (n = 3). **C)** HaCaT WT and NRF2-KO cells were treated with SFN (5  $\mu$ M) for 1, 2:30, 4, 8 or 16 h mRNA *HMOX1* and *AKR1B10* levels were analysed as described in A (n = 3). **D)** HaCaT cells were transfected with either siControl or siKEAP1. 36 h later cells were treated with either DMSO, compound 2 (10  $\mu$ M) or SFN (5  $\mu$ M) for 3 h. Cells were lysed and samples were analysed by Western Blot. Left panel is a representative Western blot and right panel shows the quantification of NRF2 protein levels against the loading control. Data represent means  $\pm$  SD (n = 2) and are expressed relative to the siControl DMSO sample; the corresponding quantifications of BACH1 and HMOX1 protein levels are shown in Suppl. Fig. S3A.



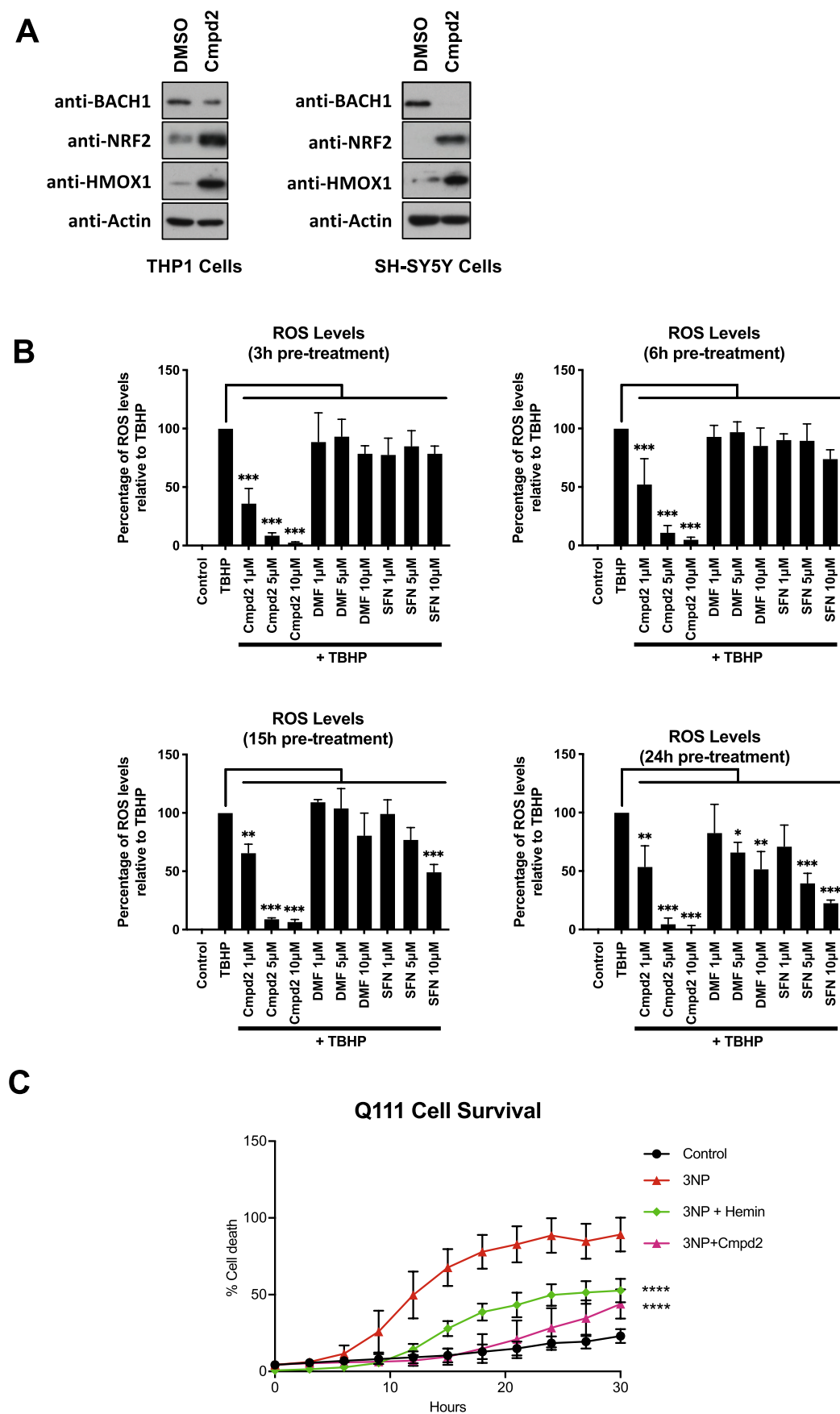


**Fig. 4.** Compound 2 stabilizes NRF2 and induces HMOX1 in macrophages and neural cells and protects cells from 3-NP mediated cytotoxicity in an *in vitro* HD model. **A)** THP1 or SH-SY5Y cells were treated with either DMSO or compound 2 (10  $\mu$ M). After 3 h, cells were lysed and BACH1, NRF2, HMOX1 and Actin protein levels were analysed by Western Blot. **B)** HaCaT cells were treated as indicated for 3h, 6h, 15h or 24h and the detection and quantification of ROS (DCF fluorescence) was measured by fluorescence microscopy. Data represent means  $\pm$  SD ( $n = 3$ ) and are expressed relative to control cells. \* $P \leq 0.05$ , \*\* $P \leq 0.01$ , \*\*\* $P \leq 0.001$ . **C)** Striatal Q111 cells were pre-treated with either DMSO, compound 2 (5  $\mu$ M) or hemin (5  $\mu$ M) for 6 h and then exposed to 10 mM 3-NP in low glucose media for an additional 24 h. Cell death was monitored using the INCUCYTE. \*\*\*\* $P \leq 0.0001$ .

Huntington's disease as models for inflammation and oxidative stress in the brain. First, we tested for target engagement in macrophage-like THP1 cells and the neuroblastoma cell line SH-SY-5Y. Compound 2 treatment efficiently decreased the levels of BACH1, induced HMOX1 and stabilised NRF2 in these cell lines (Fig. 4A). As ROS play a role in HD, and may be the initial molecules leading to apoptosis, we compared the ability of compound 2 to decrease the levels of ROS generated by treatment with *tert*-butyl hydroperoxide (tBHP) with that of SFN and dimethyl fumarate (DMF) at different time points. DMF is a NRF2 inducer that has been approved for the treatment of multiple sclerosis by the FDA. At all time points tested, compound 2 decreased the ROS levels more efficiently than either SFN or DMF (Fig. 4B). It is known that CBD is a direct antioxidant, and our results suggest that compound 2 maintains such properties. This highlights that compound 2 has three important activities, i.e. direct antioxidant, NRF2 activator and BACH1 inhibitor. Its antioxidant properties will provide acute protection (independent of cell signalling) while its effects due to NRF2 and BACH1-targeting will be slower but sustained (signalling-dependent).

Furthermore, we tested whether compound 2 could provide neuroprotection in an *in vitro* model for HD, using conditionally-immortalized striatal neuronal progenitor cell lines expressing endogenous levels of mutant huntingtin (STHdhQ111/Q111). 3-nitropropionic acid (3-NP) is a natural toxin that significantly induces oxidative damage in the brain, producing striatal lesions that are very similar to those of patients with HD [53]; and thus, it is widely used as the model agent to mimic HD. When used in the Q111 striatal neural cell line, treatment with compound 2 significantly reduced the cytotoxicity caused by 3-NP (Fig. 4C), as efficiently as hemin did, confirming its protective effect.

Our data demonstrate that O-methyl *para*-cannabidiolquinone (compound 2) has dual activity as a BACH1 inhibitor and an NRF2 activator, as well as direct antioxidant properties, which would collectively contribute to its overall cytoprotective effect. This is a very attractive profile for drugs against oxidative stress and/or inflammatory associated conditions, such as most neurodegenerative disorders, and our data on a HD cell model provide a solid rationale for future studies *in vivo* using NDs models. It is noteworthy that with aging, NRF2 signaling is impaired [54–56]. A comparison of NRF2 activation by sulforaphane in bronchial epithelial cells isolated from young human subjects (21–29 years) and older (60–69 years) individuals, non-smokers, has shown that the inducibility of the NRF2-mediated cytoprotective responses is diminished in cells from older adults [57]. Importantly, this is accompanied by an increased expression of BACH1 [57]. Conversely, silencing of BACH1 enhances sulforaphane-induced expression of NRF2-target genes in cells from older subjects [58]. Thus, our findings suggest that compounds such as compound 2 may have beneficial effects in aging.

## Funding

This work was supported by the Medical Research Institute of the University of Dundee, Cancer Research UK (C52419/A22869 and C20953/A18644) (LV and ADK), Tenovus Scotland (T18/07) (LC), and by grant RTC-2017-6109-1 from the Ministry of the Economy and Competition (MINECO) and co-financed with the European Union FEDER funds (EM).

## Authors contribution

LC, JU, MP, DM and DC conducted the experiments and were responsible for initial data analysis, figure preparation and statistical analysis. GA provided resources. LV and EM and ADK had a leading contribution in the design of the study, and an active role in the discussion and interpretation of the whole dataset. LV wrote the original draft of the manuscript. LV, EM, ADK, GA and LC, reviewed and edited the manuscript. Funding acquisition LV and EM. All the authors take full responsibility for the work.

## Declaration of competing interest

EM and GA are members of the Scientific Advisory Board of Emerald Health Biotechnology. ADK is a member of the Scientific Advisory Board of Evgen Pharma, and a consultant for Aclipse Therapeutics and Vividion Therapeutics.

## Appendix A. Supplementary data

Supplementary data to this article can be found online at <https://doi.org/10.1016/j.redox.2020.101689>.

## References

- [1] K. Itoh, et al., An Nrf2/small maf heterodimer mediates the induction of phase II detoxifying enzyme genes through antioxidant response Elements, *Biochem. Biophys. Res. Commun.* 236 (2) (Jul. 1997) 313–322, <https://doi.org/10.1006/bbrc.1997.6943>.
- [2] T. Oyake, et al., Bach proteins belong to a novel family of BTB-basic leucine zipper transcription factors that interact with MafK and regulate transcription through the NF-E2 site, *Mol. Cell Biol.* 16 (11) (Nov. 1996) 6083–6095, <https://doi.org/10.1128/MCB.16.11.6083>.
- [3] M. Furukawa, Y. Xiong, BTB protein Keap1 targets antioxidant transcription factor Nrf2 for ubiquitination by the Cullin 3-roc1 ligase, *Mol. Cell Biol.* 25 (1) (Jan. 2005) 162–171, <https://doi.org/10.1128/MCB.25.1.162-171.2005>.
- [4] K.I. Tong, A. Kobayashi, F. Katsuoka, M. Yamamoto, Two-site substrate recognition model for the Keap1-Nrf2 system: a hinge and latch mechanism, *Biol. Chem.* 387 (10) (Oct. 2006) 1311–1320, <https://doi.org/10.1515/BC.2006.164>.
- [5] K. Igarashi, T. Kurosaki, R. Roychoudhuri, BACH transcription factors in innate and adaptive immunity, *Nat. Rev. Immunol.* 17 (7) (Jul. 2017) 437–450, <https://doi.org/10.1038/nri.2017.26>.
- [6] M.D. Maines, THE HEME OXYGENASE SYSTEM: A regulator of second messenger gases, *Annu. Rev. Pharmacol. Toxicol.* 37 (1) (Apr. 1997) 517–554, <https://doi.org/10.1146/annurev.pharmtox.37.1.517>.
- [7] J.F. Reichard, G.T. Motz, A. Puga, Heme oxygenase-1 induction by NRF2 requires inactivation of the transcriptional repressor BACH1, *Nucleic Acids Res.* 35 (21) (Dec. 2007) 7074–7086, <https://doi.org/10.1093/nar/gkm638>.
- [8] J. Sun, et al., Hemoprotein Bach1 regulates enhancer availability of heme oxygenase-1 gene, *EMBO J.* 21 (19) (Oct. 2002) 5216–5224, <https://doi.org/10.1093/emboj/cdf516>.
- [9] L. Casares, et al., Cannabidiol induces antioxidant pathways in keratinocytes by targeting BACH1, *Redox Biol.* 28 (Jan. 2020) 101321, <https://doi.org/10.1016/j.redox.2019.101321>.
- [10] J.P. Roach, et al., Heme oxygenase-1 induction in macrophages by a hemoglobin-based oxygen carrier reduces endotoxin-stimulated cytokine secretion, *Shock* Augusta Ga 31 (3) (Mar. 2009) 251–257, <https://doi.org/10.1097/SHK.0b013e3181834115>.
- [11] S.-Y. Hung, H.-C. Liou, K.-H. Kang, R.-M. Wu, C.-C. Wen, W.-M. Fu, Overexpression of heme oxygenase-1 protects dopaminergic neurons against 1-methyl-4-phenylpyridinium-induced neurotoxicity, *Mol. Pharmacol.* 74 (6) (Dec. 2008) 1564–1575, <https://doi.org/10.1124/mol.108.048611>.
- [12] K. Chen, K. Gunter, M.D. Maines, Neurons overexpressing heme oxygenase-1 resist oxidative stress-mediated cell death, *J. Neurochem.* 75 (1) (Jul. 2000) 304–313, <https://doi.org/10.1046/j.1471-4159.2000.0750304.x>.
- [13] M.H. Kapturczak, et al., Heme oxygenase-1 modulates early inflammatory responses, *Am. J. Pathol.* 165 (3) (Sep. 2004) 1045–1053.
- [14] S.F. Llesuy, M.L. Tomaro, Heme oxygenase and oxidative stress. Evidence of involvement of bilirubin as physiological protector against oxidative damage, *Biochim. Biophys. Acta* 1223 (1) (Aug. 1994) 9–14, [https://doi.org/10.1016/0167-4889\(94\)90067-1](https://doi.org/10.1016/0167-4889(94)90067-1).
- [15] L.E. Otterbein, et al., Carbon monoxide has anti-inflammatory effects involving the mitogen-activated protein kinase pathway, *Nat. Med.* 6 (4) (Apr. 2000) 422–428, <https://doi.org/10.1038/74680>.
- [16] M. Zhang, B.H. Zhang, L. Chen, W. An, Overexpression of heme oxygenase-1 protects smooth muscle cells against oxidative injury and inhibits cell proliferation, *Cell Res.* 12 (2) (Jun. 2002) 123–132, <https://doi.org/10.1038/sj.cr.7290118>.
- [17] Y. Zenke-Kawasaki, et al., Heme induces ubiquitination and degradation of the transcription factor Bach1, *Mol. Cell Biol.* 27 (19) (Oct. 2007) 6962–6971, <https://doi.org/10.1128/MCB.02415-06>.
- [18] K. Igarashi, et al., Heme regulates gene expression by triggering Crm1-dependent nuclear export of Bach1, *EMBO J.* 23 (13) (Jul. 2004) 2544–2553, <https://doi.org/10.1038/sj.emboj.7600248>.
- [19] L. Lignitto, et al., Nrf2 activation promotes lung cancer metastasis by inhibiting the degradation of Bach1, *Cell* 178 (2) (Jul. 2019) 316–329, <https://doi.org/10.1016/j.cell.2019.06.003>, e18.
- [20] S.R. Robinson, T.N. Dang, R. Dringen, G.M. Bishop, Hemin toxicity: a preventable source of brain damage following hemorrhagic stroke, *Redox Rep.* 14 (6) (Dec. 2009) 228–235, <https://doi.org/10.1179/135100009X12525712409931>.
- [21] D.M. Elliott, N. Singh, M. Nagarkatti, P.S. Nagarkatti, Cannabidiol attenuates experimental autoimmune encephalomyelitis model of multiple sclerosis through induction of myeloid-derived suppressor cells, *Front. Immunol.* 9 (Aug. 2018) 1782, <https://doi.org/10.3389/fimmu.2018.01782>.

- [22] F.F. Peres, A.C. Lima, J.E.C. Hallak, J.A. Crippa, R.H. Silva, V.C. Abílio, Cannabidiol as a promising strategy to treat and prevent movement disorders? *Front. Pharmacol.* 9 (May 2018) 482, <https://doi.org/10.3389/fphar.2018.00482>.
- [23] O.C. Attucks, et al., Induction of heme oxygenase 1 (HMOX1) by HPP-4382: a novel modulator of Bach1 activity, *PloS One* 9 (7) (Jul. 2014), <https://doi.org/10.1371/journal.pone.0101044>.
- [24] A. Cuadrado, et al., Therapeutic targeting of the NRF2 and KEAP1 partnership in chronic diseases, *Nat. Rev. Drug Discov.* 18 (4) (Apr. 2019) 295–317, <https://doi.org/10.1038/s41573-018-0008-x>.
- [25] A.T. Dinkova-Kostova, R.V. Kostov, P. Canning, Keap1, the cysteine-based mammalian intracellular sensor for electrophiles and oxidants, *Arch. Biochem. Biophys.* 617 (Mar. 2017) 84–93, <https://doi.org/10.1016/j.abb.2016.08.005>.
- [26] N. Robledinos-Antón, R. Fernández-Ginés, G. Manda, A. Cuadrado, Activators and inhibitors of NRF2: a review of their potential for clinical development, *Oxid. Med. Cell. Longev.* 2019 (Jul. 2019) 1–20, <https://doi.org/10.1155/2019/9372182>.
- [27] Q. Ma, Role of Nrf2 in oxidative stress and toxicity, *Annu. Rev. Pharmacol. Toxicol.* 53 (1) (2013) 401–426, <https://doi.org/10.1146/annurev-pharmtox-011112-140320>.
- [28] A.C. Wild, H.R. Moinova, R.T. Mulcahy, Regulation of gamma-glutamylcysteine synthetase subunit gene expression by the transcription factor Nrf2, *J. Biol. Chem.* 274 (47) (Nov. 1999) 33627–33636, <https://doi.org/10.1074/jbc.274.47.33627>.
- [29] E.H. Kobayashi, et al., Nrf2 suppresses macrophage inflammatory response by blocking proinflammatory cytokine transcription, *Nat. Commun.* 7 (1) (Sep. 2016) 11624, <https://doi.org/10.1038/ncomms11624>.
- [30] B.E. Townsend, R.W. Johnson, Sulforaphane induces Nrf2 target genes and attenuates inflammatory gene expression in microglia from brain of young adult and aged mice, *Exp. Gerontol.* 73 (Jan. 2016) 42–48, <https://doi.org/10.1016/j.exger.2015.11.004>.
- [31] R.A. Floyd, Neuroinflammatory processes are important in neurodegenerative diseases: an hypothesis to explain the increased formation of reactive oxygen and nitrogen species as major factors involved in neurodegenerative disease development, *Free Radic. Biol. Med.* 26 (9) (May 1999) 1346–1355, [https://doi.org/10.1016/S0891-5849\(98\)00293-7](https://doi.org/10.1016/S0891-5849(98)00293-7).
- [32] M. Brandes, N.E. Gray, NRF2 as a therapeutic target in neurodegenerative diseases, *ASN NEURO* 12 (Jan. 2020), <https://doi.org/10.1177/1759091419899782>.
- [33] R. Bomprezzi, 'Dimethyl fumarate in the treatment of relapsing–remitting multiple sclerosis: an overview', *Ther. Adv. Neurol. Disord.* 8 (1) (Jan. 2015) 20–30, <https://doi.org/10.1177/1756285614564152>.
- [34] P. McColgan, S.J. Tabrizi, 'Huntington's disease: a clinical review', *Eur. J. Neurol.* 25 (1) (Jan. 2018) 24–34, <https://doi.org/10.1111/ene.13413>.
- [35] L. Quinti, et al., 'KEAP1-modifying small molecule reveals muted NRF2 signaling responses in neural stem cells from Huntington's disease patients', *Proc. Natl. Acad. Sci. Unit. States Am.* 114 (23) (Jun. 2017) E4676–E4685, <https://doi.org/10.1073/pnas.1614943114>.
- [36] G. Ellrichmann, et al., 'Efficacy of fumaric acid esters in the R6/2 and YAC128 models of Huntington's disease', *PloS One* 6 (1) (Jan. 2011) e16172, <https://doi.org/10.1371/journal.pone.0016172>.
- [37] A.K. MacLeod, et al., 'Characterization of the cancer chemopreventive NRF2-dependent gene battery in human keratinocytes: demonstration that the KEAP1–NRF2 pathway, and not the BACH1–NRF2 pathway, controls cytoprotection against electrophiles as well as redox-cycling compounds', *Carcinogenesis* 30 (9) (Sep. 2009) 1571–1580, <https://doi.org/10.1093/carcin/bgp176>.
- [38] D. Del Prete, et al., Turmeric sesquiterpenoids: expeditious resolution, comparative bioactivity, and a new bicyclic turmeronoid, *J. Nat. Prod.* 79 (2) (Feb. 2016) 267–273, <https://doi.org/10.1021/acs.jnatprod.5b00637>.
- [39] I.M. Munoz, P. Szytniarowski, R. Toth, J. Rouse, C. Lachaud, Improved genome editing in human cell lines using the CRISPR method, *PloS One* 9 (10) (Oct. 2014), e109752, <https://doi.org/10.1371/journal.pone.0109752>.
- [40] Z. Niatetskaya, et al., 'HIF prolyl hydroxylase inhibitors prevent neuronal death induced by mitochondrial toxins: therapeutic implications for Huntington's disease and Alzheimer's disease', *Antioxidants Redox Signal.* 12 (4) (Feb. 2010) 435–443, <https://doi.org/10.1089/ars.2009.2800>.
- [41] O. Tagliatalata-Scafati, et al., Cannabimovone, a cannabinoid with a rearranged terpenoid skeleton from hemp, *Eur. J. Org. Chem.* 2010 (11) (Apr. 2010) 2067–2072, <https://doi.org/10.1002/ejoc.200901464>.
- [42] D. Caprioglio, et al., The oxidation of phytocannabinoids to cannabinoquinoids, *J. Nat. Prod.* 83 (5) (May 2020) 1711–1715, <https://doi.org/10.1021/acs.jnatprod.9b01284>.
- [43] D. Caprioglio, et al., O-methyl phytocannabinoids: semi-synthesis, analysis in Cannabis flowerheads, and biological activity, *Planta Med.* 85 (11/12) (Aug. 2019) 981–986, <https://doi.org/10.1055/a-0883-5383>.
- [44] F. Trettel, et al., Dominant phenotypes produced by the HD mutation in STHdhQ111 striatal cells, *Hum. Mol. Genet.* 9 (19) (Nov. 2000) 2799–2809, <https://doi.org/10.1093/hmg/9.19.2799>.
- [45] J.W. Fahey, A.T. Dinkova-Kostova, K.K. Stephenson, P. Talalay, 'The "prochaska" microtiter plate bioassay for inducers of NQO1', in: *Methods in Enzymology*, vol. 382, Academic Press, 2004, pp. 243–258.
- [46] H.J. Prochaska, M.J. De Long, P. Talalay, On the mechanisms of induction of cancer-protective enzymes: a unifying proposal, *Proc. Natl. Acad. Sci. U. S. A.* 82 (23) (Dec. 1985) 8232–8236.
- [47] A.T. Dinkova-Kostova, P. Talalay, NAD(P)H:quinone acceptor oxidoreductase 1 (NQO1), a multifunctional antioxidant enzyme and exceptionally versatile cytoprotector, *Arch. Biochem. Biophys.* 501 (1) (Sep. 2010) 116–123, <https://doi.org/10.1016/j.abb.2010.03.019>.
- [48] V. Zoete, M. Rougée, A.T. Dinkova-Kostova, P. Talalay, R.V. Bensasson, Redox ranking of inducers of a cancer-protective enzyme via the energy of their highest occupied molecular orbital, *Free Radic. Biol. Med.* 36 (11) (Jun. 2004) 1418–1423, <https://doi.org/10.1016/j.freeradbiomed.2004.03.008>.
- [49] R.V. Bensasson, V. Zoete, A.T. Dinkova-Kostova, P. Talalay, Two-step mechanism of induction of the gene expression of a prototypic cancer-protective enzyme by diphenols, *Chem. Res. Toxicol.* 21 (4) (Apr. 2008) 805–812, <https://doi.org/10.1021/tx7002883>.
- [50] X.J. Wang, J.D. Hayes, L.G. Higgins, C.R. Wolf, A.T. Dinkova-Kostova, Activation of the NRF2 signaling pathway by copper-mediated redox cycling of para- and ortho-hydroquinones, *Chem. Biol.* 17 (1) (Jan. 2010) 75–85, <https://doi.org/10.1016/j.chembiol.2009.12.013>.
- [51] T. Satoh, S.R. McKercher, S.A. Lipton, Nrf2/ARE-mediated antioxidant actions of pro-electrophilic drugs, *Free Radic. Biol. Med.* 65 (Dec. 2013) 645–657, <https://doi.org/10.1016/j.freeradbiomed.2013.07.022>.
- [52] K. Wu, P. McDonald, J. Liu, C. Klaassen, Screening of natural compounds as activators of the keap1–Nrf2 pathway, *Planta Med.* 80 (Dec. 2013) 97–104, <https://doi.org/10.1055/s-0033-1351097>, 01.
- [53] G.W. Kim, P.H. Chan, Involvement of superoxide in excitotoxicity and DNA fragmentation in striatal vulnerability in mice after treatment with the mitochondrial toxin, 3-nitropropionic acid, *J. Cerebr. Blood Flow Metabol.* 22 (7) (Jul. 2002) 798–809, <https://doi.org/10.1097/00004647-200207000-00005>.
- [54] M.M. Sachdeva, M. Cano, J.T. Handa, Nrf2 signaling is impaired in the aging RPE given an oxidative insult, *Exp. Eye Res.* 119 (Feb. 2014) 111–114, <https://doi.org/10.1016/j.exer.2013.10.024>.
- [55] M.N. Valcarcel-Ares, et al., Disruption of Nrf2 signaling impairs angiogenic capacity of endothelial cells: implications for microvascular aging, *J. Gerontol. A. Biol. Sci. Med. Sci.* 67 (8) (Aug. 2012) 821–829, <https://doi.org/10.1093/gerona/glr229>.
- [56] L.C.D. Pomatto, et al., 'Aging attenuates redox adaptive homeostasis and proteostasis in female mice exposed to traffic-derived nanoparticles ("vehicular smog")', *Free Radic. Biol. Med.* 121 (Jun. 2018) 86–97, <https://doi.org/10.1016/j.freeradbiomed.2018.04.574>.
- [57] L. Zhou, H. Zhang, K.J.A. Davies, H.J. Forman, Aging-related decline in the induction of Nrf2-regulated antioxidant genes in human bronchial epithelial cells, *Redox Biol.* 14 (Apr. 2018) 35–40, <https://doi.org/10.1016/j.redox.2017.08.014>.
- [58] H. Zhang, L. Zhou, K.J.A. Davies, H.J. Forman, Silencing Bach1 alters aging-related changes in the expression of Nrf2-regulated genes in primary human bronchial epithelial cells, *Arch. Biochem. Biophys.* 672 (Sep. 2019) 108074, <https://doi.org/10.1016/j.abb.2019.108074>.